IEEE Access
Multidisciplinary : Rapid Review : Open Access Journal

Received January 9, 2022, accepted January 19, 2022, date of publication January 25, 2022, date of current version January 28, 2022.

Digital Object Identifier 10.1109/ACCESS.2022.3145985

Application of Decomposition and Coordination Optimization Methodology in Reliability Allocation of Systems

BIN BAI[1,2], CHUXIONG XIE[1], XIANGDONG LIU[1], WEI LI[1], AND WEIYU ZHONG[1]

[1]Hunan Sany Polytechnic College, Changsha 410100, China
[2]Science and Technology on Particle Transport Separation Laboratory, Institute of Physical and Chemical Engineering of Nuclear Industry, Tianjin 300180, China

Corresponding author: Bin Bai (baibin@126.com)

This work was supported in part by the Scientific Research Project of the Hunan Education Department under Grant 21C1235, in part by the National Natural Science Foundation of Hebei Province under Grant E2020202217, and in part by the Open Research Fund for Key Laboratory of National Defense Science and Technology for Particle Transport and Enrichment Technology under Grant STPTS202111.

ABSTRACT A decomposition-coordination optimization method termed as analytical target cascading-based exterior penalty function (ATC-EPF) is proposed to investigate the reliability allocation aiming at the low computational efficiency for large complex systems. Firstly, the optimization model is established via ATC-EPF, which is decomposed into the models of subsystems. Then the subsystems are calculated in parallel, which reduces the computational cost greatly in the condition of keeping the computational accuracy. The results are fine which are verified by two study cases including one numerical case and one engineering case. This research is of great significance to large-scale system planning and design.

INDEX TERMS Analytical target cascading, optimization, exterior penalty function, reliability, computational efficiency.

I. INTRODUCTION

Generally, a system is defined as a composed of several units with specific functions. It is expected to find an optimal design scheme that can meet different requirements in terms of engineering system. At present, there are two kinds of methods, one is direct solution method, the other is the decomposed coordination method. The direct solution method is to comprehensively consider the design of each subsystem and design unit as well as their coupling relationship, and directly search the optimal solution in the design space of the system. However, this method will face with the difficulty that the solution scale and calculation amount will multiply with the increase of the complexity due to the high dimension, multivariable and complex coupling characteristics of the system. Thus, the general optimization methods must be improved to solve the large-scale optimization problems. Generally, there are two ways to optimize a large-complicated system, namely, decomposition and coordination method (DCM) and analytical target cascading (ATC). Though, DCM can improve the computational efficiency or minimize the cost for the systems, there are some shortcomings in design theory. However, the ATC method can not only reduce the computational cost but also improve the optimization accuracy. Furthermore, the ATC can be used to study the reliability of large-scale engineering optimization.

DCM is suitable for large-scale system optimization design [1]–[3]. It decomposes the system into several sub-programmings and a master programming for global coordination, such as large-scale railway networks, multi-rotor Unmanned Aerial Vehicle, and multi-scale coupled ecological system, etc. The bi-level optimal planning model was investigated to determine the optimal location of energy storage systems and capacity in a virtual power plant or illustrate the performance of the proposed framework by robotics [4], [5]. Some other schemes were researched such as stochastic dual dynamic parallel programming [6], Dantzig Wolfe decomposition algorithms [7], and the distributed local selfish optimization models [8], to deal with high-dimensional state-spaces and optimize power generation

The associate editor coordinating the review of this manuscript and approving it for publication was Zhaojun Steven Li.

planning or large-scale block angular linear programming. In addition, probabilistic distributed assessments or nonlinear programing [9]–[11] were studied via decomposition and coordination approach. All of these investigations improved the computational efficiency or minimized the cost for the systems [12]–[14]. However, there are some shortcomings in design for the DCM.

In order to solve the shortcomings in design theory, ATC method was introduced, which was first proposed by Kim [15] as an object-based general model to handle the optimization problem of hierarchical structure system. Later, the scientific research team led by Professor Papalambros conducted in-depth discussion on this model, and proposed a series of solving methods. The significant feature of ATC is that large-scale systems can be decomposed into subsystems to improve computational efficiency and keep the cost to a minimum, thus this method has been widely used in engineering practices. For instance, wind farm cluster, active distribution network, virtual micro-grid levels, multiregional power systems and synchronous machine were investigated by ATC [16]–[18], which solved the optimal control problems and time properties. This method was also widely used in the research of vehicle systems, especially the suspension system such as high-speed trains, commercial vehicle, and the integrated automobile chassis system [19]–[22]. In addition, some researchers investigated the green design problem of complex engineering system [23]–[25], configuring assembly supply chains including several enterprises, which expanded the scope of production services [26]. These investigations achieve the consistency and optimality for overall system in industrial practices. The results provide valuable insights in the feasibility of system-level design targets and the adequacy of subproblem design spaces during product development. Furthermore, the ATC method reduces the computational cost and improves the optimization accuracy.

To address the convergence efficiency for large-scale engineering optimization problems, ATC was improved by researchers, e.g., the linear and the proximal cutting plane methods were developed to reduce the number of iterations and function evaluations [27]. The accelerated and robust ATC was presented to solve the optimal power flow distributedly [28]. The collaborative planning method was used to optimize the distributed power supply for the distribution network [29]. In addition, alternating direction with parallelization in non-hierarchical ATC [30], nonlinear convex and non-convex ATC [31], nonhierarchical target-response coupling between subproblems functions [32] were studied, which could significantly reduce the number of iterations and solve the problem of slow convergence, oscillation around the optimal point, divergence or unbalance of objective terms. The original all-at-once constrained optimization problem is decomposed into a hierarchical system. The objective function is combined with the consistency constraints in each element. Also, these methodologies can parallelize the subproblem optimizations, which are implemented in conjunction with augmented Lagrangian coordination for ATC-decomposed problems.

Practically, many influencing factors were uncertain, some scholars studied the reliability of large-scale engineering optimization problems-based ATC. The probabilistic ATC was combined with first-order reliability assessment algorithms to estimate the statistical performance of the subsystems, modules, components, and address the uncertainties efficiently in investigating the concurrent and consistent design [33]–[39]. Considering the impacts of variability and uncertainty in design variables, the probabilistic ATC can calculate the probabilistic characteristic of the interrelated responses and linking variables, also, it can solve the reliability allocation problems for large scale system and deal with the matching of the high order moments for the multilevel design with non-normal interrelated responses. The probabilistic optimization problem was converted into an equivalent deterministic optimization problem, then hierarchically decomposed them into subproblems. The computational efficiency is remarkably improved. In addition, some researchers considered the interval uncertainty and researched the complex system with the maximum variation analysis-based ATC, and optimized all the subsystems autonomously to search the robust optimal solution [40]. The above investigations manifest the most of the optimization problems are separable in decomposition and coordination methods, which have certain limitations. Based on this, the ATC is improved, i.e., analytical target cascading based on exterior penalty function (ATC-EPF), to investigate the reliability allocation of larger complex engineering optimization.

This decomposition-coordination optimization method is attractive for complex and large-scale systems in industrial practices. The EPF formulation is implemented using double-loop (EPF I) and single-loop (EPF II) coordination strategies, and two penalty-parameter-updating schemes. The decomposed subsystem can be calculated in parallel, which can accurately and efficiently determine the optimal capacities with large quantities of stochastic scenarios, and reduce the computational cost observably to achieve overall system consistency and optimality.

II. RELATED WORK

Generally, the hierarchical structure of system is described by the classical ATC model, as Fig. 1.

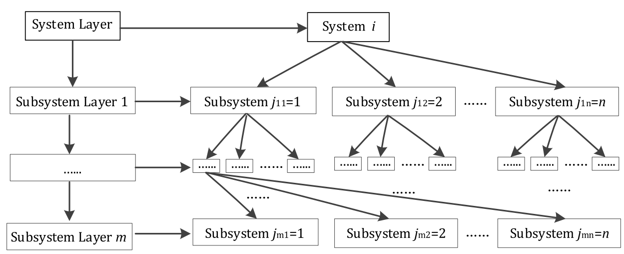

FIGURE 1. System hierarchical structure of ATC model.

The optimization problems of system described by Fig. 1, which can be written as

$$\begin{aligned} &\min \left\| \boldsymbol{R}_{\text{sys}}(\boldsymbol{x}) - \mathbf{T} \right\| \\ &s.t\ \boldsymbol{g}(\boldsymbol{x}) \le \mathbf{0} \end{aligned} \tag{1}$$

where $\mathbf{T}$ is the target of system, $\boldsymbol{R}_{\text{sys}}(\boldsymbol{x})$ is the response function of system, $\boldsymbol{g}(\boldsymbol{x})$ is the constraint function of system, $\boldsymbol{x}$ is the vector of system.

The optimization goal is to minimize the difference between the $\boldsymbol{R}_{\text{sys}}(\boldsymbol{x})$ and $\mathbf{T}$ under the constraint condition $\boldsymbol{g}(\boldsymbol{x}) \le \mathbf{0}$. This optimization model is called All in One (AIO) model, which is the initial model of system optimization. However, it is very difficult to solve such a model using the direct solution method for complex systems. In this work, based on the idea of decomposition coordination optimization, the objectives of each subsystem are imported into AIO model to decompose the original optimization model, which is called Analytical Target Cascading-based Exterior Penalty Function (ATC-EPF).

Firstly, the response function is expressed as

$$\boldsymbol{R} = (\boldsymbol{R}_1, \boldsymbol{R}_2, \boldsymbol{R}_3, \cdots, \boldsymbol{R}_n)^{\mathrm{T}} \tag{2}$$

$$\boldsymbol{R}_j = \boldsymbol{r}_j(\boldsymbol{x}_j, \boldsymbol{y}_j), \quad j = 1, 2, \cdots, n \tag{3}$$

$$\boldsymbol{y} = \boldsymbol{y}_j, \quad j = 1, 2, \cdots, n \tag{4}$$

The optimization model of Eq. (1) is rewritten as

$$\begin{aligned} &\min \left\| \boldsymbol{R}_{\text{sys}}(\boldsymbol{x}_{\text{sys}}, \boldsymbol{R}_{j\in\mathcal{E}}, \boldsymbol{y}) - \mathbf{T} \right\| \\ &s.t\ \boldsymbol{g}_{sys}(\boldsymbol{x}_{\text{sys}}, \boldsymbol{R}, \boldsymbol{y}) \le \mathbf{0}, \quad j \in \mathcal{E}; \\ &\quad \boldsymbol{g}_j(\boldsymbol{x}_j, \boldsymbol{y}_j) \le \mathbf{0}, \quad j \in \mathcal{E} \\ &\quad \boldsymbol{R}_j = \boldsymbol{R}_j^l, \quad j \in \mathcal{E}; \\ &\quad \boldsymbol{y} = \boldsymbol{y}_j, \quad j \in \mathcal{E}; \end{aligned} \tag{5}$$

where $\boldsymbol{g}_{sys}$ is the constraint function of system, $\boldsymbol{g}_j$ is the constraint function of the jth subsystem, $\boldsymbol{x}_{\text{sys}}$ is the local design variables at system, $\boldsymbol{x}_j$ is the local design variable of the jth subsystem, $\boldsymbol{r}_j(\boldsymbol{x}_j, \boldsymbol{y}_j)$ is the response function of the jth system, which is expressed by $\boldsymbol{R}_j^l$ at the subsystem layer and by $\boldsymbol{R}_j$ at the system layer. $\boldsymbol{y}_j$ is the connection variable corresponding to the jth subsystem, which is expressed by $\boldsymbol{y}$ at system, ε represents the set of all subsystems, where the number of elements is n.

The equation constraint in Eq. (5) is introduced into the objective function, the optimization model is denoted as

$$\begin{aligned} &\min \left\{ \left\| \boldsymbol{R}_{sys}(\boldsymbol{x}_{\text{sys}}, \boldsymbol{R}_{j\in\mathcal{E}}, \boldsymbol{y}) - \mathbf{T} \right\| + \frac{\sigma}{2} \left(\sum_{j\in\mathcal{E}} \left\| \boldsymbol{R}_j - \boldsymbol{R}_j^l \right\|_2^2 + \sum_{j\in\mathcal{E}} \left\| \boldsymbol{y} - \boldsymbol{y}_j \right\|_2^2 \right) \right\} \\ &s.t\ \boldsymbol{g}_{sys}(\boldsymbol{x}_{sys}, \boldsymbol{R}_j, \boldsymbol{y}) \le \mathbf{0} \\ &\quad \boldsymbol{g}_j(\boldsymbol{x}_j, \boldsymbol{y}_j) \le \mathbf{0}, \quad j \in \mathcal{E} \end{aligned} \tag{6}$$

where σ is penalty factor.

Then, the original system is decomposed into two parts, one is the master programming at system layer, and the other is the sub-programming at subsystem layer.

The master programming is described as

$$\begin{aligned} &\min \left\{ \left\| \boldsymbol{R}_{\text{sys}}(\boldsymbol{x}_{\text{sys}}, \boldsymbol{R}, \boldsymbol{y}) - \mathbf{T} \right\| + \frac{\sigma}{2} \left(\sum_{j\in\mathcal{E}} \left\| \boldsymbol{R}_j - \boldsymbol{r}_j(\boldsymbol{x}_j, \boldsymbol{y}_j) \right\|_2^2 + \sum_{j\in\mathcal{E}} \left\| \boldsymbol{y} - \boldsymbol{y}_j \right\|_2^2 \right) \right\} \\ &s.t\ \boldsymbol{g}_{sys}(\boldsymbol{x}_{\text{sys}}, \boldsymbol{R}, \boldsymbol{y}) \le \mathbf{0} \end{aligned} \tag{7}$$

The sub-programming of the jth subsystem is expressed as

$$\begin{aligned} &\min \left\{ \left\| \boldsymbol{R}_j - \boldsymbol{R}_j^l \right\| + \left\| \boldsymbol{y} - \boldsymbol{y}_j \right\| \right\} \\ &s.t\ \boldsymbol{g}_j(\boldsymbol{x}_j, \boldsymbol{y}_j) \le \mathbf{0}, \quad j \in \mathcal{E} \\ &\quad \boldsymbol{R}_j^l = \boldsymbol{r}_j(\boldsymbol{x}_j, \boldsymbol{y}_j) \end{aligned} \tag{8}$$

The computational procedure of master programming and sub-programming is as follow:

(1) The master programming in Eq. (7) is solved and the $\left(\boldsymbol{x}_{\text{sys}}^{(k)}, \boldsymbol{R}^{(k)}, \boldsymbol{y}^{(k)}\right)$ is obtained, where $\sigma^{(k)}$ is given, and $\boldsymbol{R}_j^l$, $\boldsymbol{y}_j$ are, respectively, as the parameter values of the master programming.

(2) The $\left(\boldsymbol{R}_j^{(k)}, \boldsymbol{y}^{(k)}\right)$ is passed to the jth ($j \in \mathcal{E}$) sub-programming, then the sub-programming is calculated, and $\left(\boldsymbol{x}_j^{(k)}, \boldsymbol{y}_j^{(k)}, \boldsymbol{R}_j^{l(k)}\right)$ is obtained.

(3) Order $\boldsymbol{\epsilon}_{\boldsymbol{R}} = \left(\boldsymbol{\epsilon}_{\boldsymbol{R}_1}, \boldsymbol{\epsilon}_{\boldsymbol{R}_2}, \cdots, \boldsymbol{\epsilon}_{\boldsymbol{R}_n}\right)^{\mathrm{T}}$, and $\boldsymbol{\epsilon}_{\boldsymbol{y}} = \left(\boldsymbol{\epsilon}_{\boldsymbol{y}_1}, \boldsymbol{\epsilon}_{\boldsymbol{y}_2}, \cdots, \boldsymbol{\epsilon}_{\boldsymbol{y}_n}\right)^{\mathrm{T}}$, then $\boldsymbol{\epsilon}_{\boldsymbol{R}_j}^{(\mathrm{k})} = \boldsymbol{R}_j^{(\mathrm{k})} - \boldsymbol{R}_j^{l(k)}$ and $\boldsymbol{\epsilon}_{\boldsymbol{y}_j}^{(\mathrm{k})} = \boldsymbol{y}^{(\mathrm{k})} - \boldsymbol{y}_j^{(\mathrm{k})}$, ($j \in \mathcal{E}$) are calculated. Next, the loop is exited and optimization results are outputted if $\left\|\boldsymbol{\epsilon}_{\boldsymbol{R}}\right\| \le \varepsilon$ and $\left\|\boldsymbol{\epsilon}_{\boldsymbol{y}}\right\| \le \varepsilon$, otherwise, go to step (4).

(4) The penalty factor $\sigma^{(k+1)} = \beta\sigma^{(k)}, \beta > 1$ is renewaled. Order $k = k + 1$ and return to step (1).

The calculation process is shown in Fig. 2.

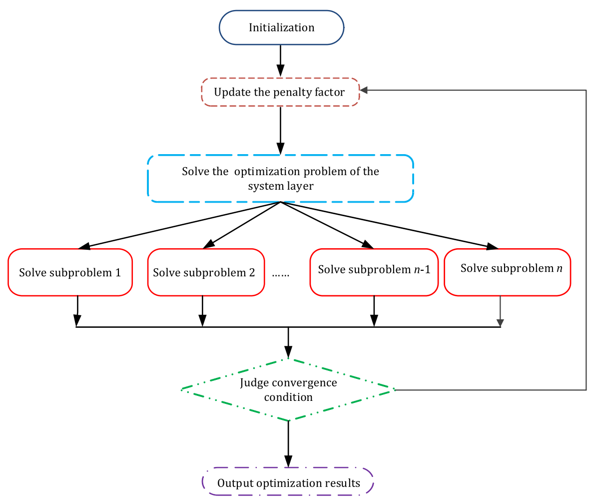

FIGURE 2. Flow chart of ATC-EPF-based penalty function.

The relationship of master programming and sub-programming is shown in Fig. 3.

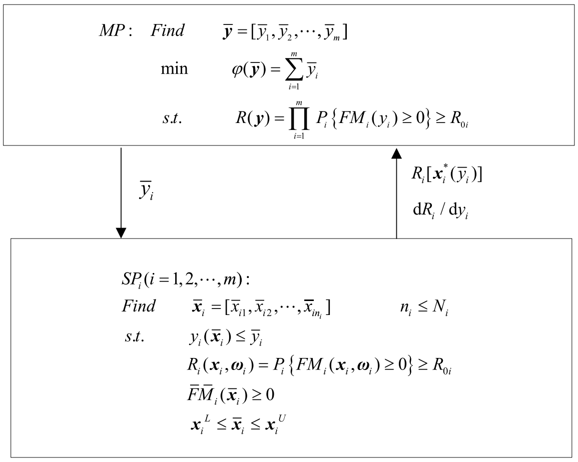

FIGURE 3. Flow chart of reliability optimization in random constraint. Notice: MP: master programming, SP_i: sub-programming, $R_i[x_i^*(\bar{y}_i)]$ is the reliability of the optimal solution x_i^* and dR_i/dy_i is the derivative of the reliability R_i. n_i is the number of random variables. $FM_i(x_i)$ is the limit state equation, $R_i(x_i, \omega_i)$ is reliability function and R_{0i} is the reliability level. x_i^L is the random variable composed by lower limit value and x_i^U is the random variable composed by upper limit value. $y_i(x_i, \omega_i)$ is the function, P_i is the reliability.

Fig. 3 indicates that the optimization model is converted into the master planning optimization model and m separable planning optimization models. The main system is assigned to each component by master planning and the assigned system is obtained by the ith sub-programming, then the optimization solution is back to the master planning. According to the return value, the system is redistributed by master planning until the output results is convergent and the optimal value is matched with the actual requirements.

However, the constraint is the random in the ith sub-programming, which needs to be transformed into the deterministic constraint. The planning idea is introduced to optimize system reliability considering other constraints in the condition of minimizing subsystem. Every subsystem is optimized but finally achieve the purpose of optimization for the whole system, and the computational efficiency of system via ATC-EPF are greatly improved.

The $R_i(\boldsymbol{x}_i, \boldsymbol{\omega}_i)$ of the ith subsystem is expressed as

$$R_i(\boldsymbol{x}_i, \boldsymbol{\omega}_i) = P_i\{FM_i(\boldsymbol{x}_i, \boldsymbol{\omega}_i) \geq 0)\} = \frac{1}{\sqrt{2\pi}} \int_{-\infty}^{-\frac{\mu_{FM_i}}{\sigma_{FM_i}}} e^{-\frac{t^2}{2}} dt \tag{9}$$

The flow chart of system by ATC-EPF is further described in Fig. 4.

The solution procedure of the ATC-EPF is shown in Fig. 5. where $\bar{M}_i^{(0)}$ is the ith initial subsystem, ε_1 is the convergent tolerances of $\left\|\bar{x}_i^{(l+1)} - \bar{x}_i^{(l)}\right\|$, ε_2 is the convergent tolerances of $\left\|\bar{M}_i^{(t+1)} - \bar{M}_i^{(t)}\right\|$, and $0 < \varepsilon_1 < 0.0015, 0 < \varepsilon_2 < 0.0012$.

Fig. 5 indicates that the reliability optimization is an iterative process of master planning and separable planning until the output values satisfy the actual requirements.

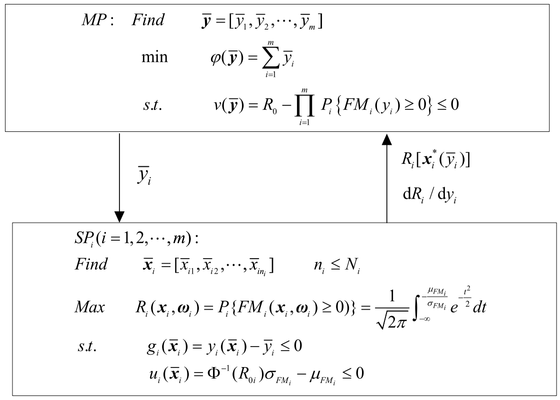

FIGURE 4. Flow chart of reliability optimization in deterministic constraint. Notice: μ_{FM_i} and σ_{FM_i} are the mean and standard deviation, $g_i(\bar{x}_i)$ and $u_i(\bar{x}_i)$ are the deterministic constraint functions.

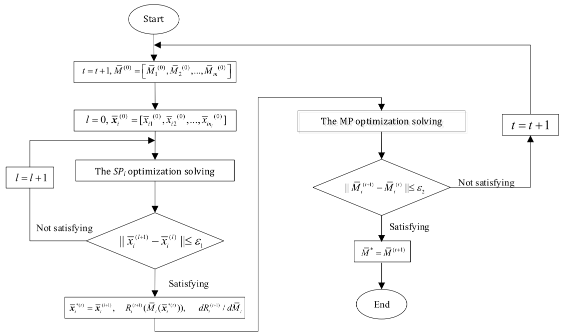

FIGURE 5. Solution procedure via ATC-EPF.

However, ATC-EPF method can reduce dimensions and improve computational efficiency and accuracy.

III. CASE STUDIES

A. NUMERICAL CASE

In order to verify the calculation accuracy and efficiency of the ATC-EPF, firstly, a numerical case is given. This is a quadratic function optimization problem including 14 design variables, 6 inequality constraints and 4 equality constraints, and all design variables are required non-negatively. The optimization model is expressed as

$$\begin{aligned}
\min f &= x_1^2 + x_2^2 \\
\text{s.t } g_1 &= x_3^{-2} + x_4^2 - x_5^2 \leq 0 \\
g_2 &= x_5^2 + x_6^{-2} - x_7^2 \leq 0 \\
g_3 &= x_8^2 + x_9^2 - x_{11}^2 \leq 0 \\
g_4 &= x_8^{-2} + x_{10}^2 - x_{11}^2 \leq 0 \\
g_5 &= x_{11}^2 + x_{12}^{-2} - x_{13}^2 \leq 0 \\
g_6 &= x_{11}^2 + x_{12}^2 - x_{14}^2 \leq 0 \\
h_1 &= x_1^2 - x_3^2 - x_4^{-2} - x_5^2 = 0 \\
h_2 &= x_2^2 - x_5^2 - x_6^2 - x_7^2 = 0 \\
h_3 &= x_3^2 - x_8^2 - x_9^{-2} - x_{10}^{-2} - x_{11}^2 = 0 \\
h_4 &= x_6^2 - x_{11}^2 - x_{12}^2 - x_{13}^2 - x_{14}^2 = 0 \\
& x_1, x_2, \cdots, x_{14} \geq 0
\end{aligned}$$

This optimization can be expressed by ATC-EPF according to Eqs. (6-8), as shown in Fig.6. The results of optimal value obtained by AIO and ATC-EPF are compared, as Table 1.

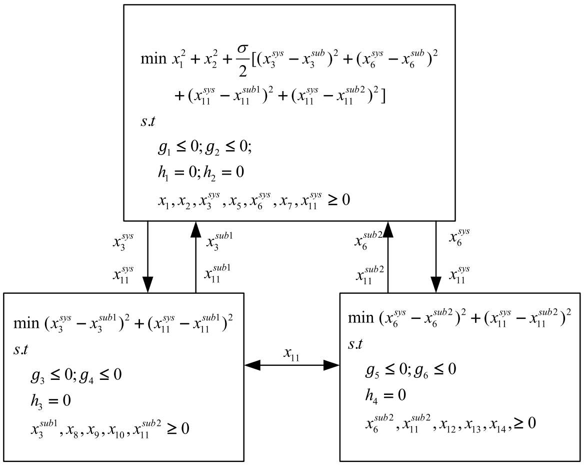

FIGURE 6. Optimization model of numerical case by ATC-EPF.

TABLE 1. Comparison of AIO method and ATC-EPF method in numerical case.

	AIO	ATC-EPF	Rate of deviation /%
x_1	2.8355	2.8858	1.77
x_2	3.0901	3.0238	2.14
x_3	2.3559	2.4174	2.61
x_4	0.7598	0.7587	0.14
x_5	0.8704	0.8641	0.72
x_6	2.8120	2.7418	2.49
x_7	0.9402	0.9379	0.24
x_8	0.9719	0.9795	0.78
x_9	0.8651	0.8374	3.20
x_{10}	0.7965	0.7744	2.77
x_{11}	1.3012	1.2606	3.12
x_{12}	0.8409	0.8403	0.07
x_{13}	1.7627	1.7281	1.96
x_{14}	1.5492	1.5097	2.54
f	17.5887	17.4716	0.67
Iterations	298	12	95.97

It is seen from Table 1 the rate of deviation via ATC-EPF compared with that of AIO is 0.07%-3.20% and the rate of deviation of the minimum function is 0.67% obtained by ATC-EPF compared with that of AIO, which satisfy the accuracy requirement. Thus, the optimal solution obtained by ATC-EPF is consistent with that of obtained by AIO, which verifies the accuracy of this method. In addition, the computational efficiency of ATC-EPF is improved 95.97% compared with that of AIO. Thus, the computational efficiency of ATC-EPF is significantly improved compared with AIO in the condition of satisfying the computational accuracy.

B. ENGINEERING CASE

The reliable product is very important for society, and reasonable reliability index allocation is of great significance to the life span. It is known the computational cost of reliability is expensive, thus ATC-EPF is adopted to calculate the reliability index allocation of products in this work. It is required to minimize the cost of the system in the condition of satisfying the constraint of reliability index. The block diagram of system is shown in Fig. 7. This large system contains 5 subsystems, which contains two components. The optimization model is as follow:

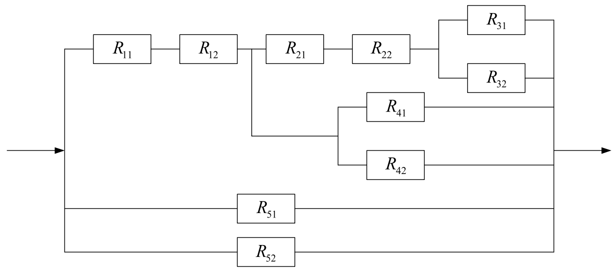

FIGURE 7. Structure block diagram of system.

$$\min C_S = \sum_{i=1}^{5}\sum_{j=1}^{2} C_{ij}$$

$$\text{s.t } R_S \ge 0.999$$

$$R_s = R_5 + R_1\left(1 - R_5\right)\left(R_2R_3 + R_4 - R_2R_3R_4\right)$$

$$0.5 \le R_{ij} \le 0.98, \quad i = 1, 2;\ j = 1, 2$$

$$0.2 \le R_{ij} \le 0.99, \quad i = 3, 4, 5;\ j = 1, 2$$

$$R_i = R_{i1}R_{i2} \ge 0.5, \quad i = 1, 2$$

$$0.5 \le \mathrm{R_i} \le 0.998, \quad i = 3, 4, 5$$

$$R_i = 1 - \left(1 - R_{i1}\right)\left(1 - R_{i2}\right), \quad i = 3, 4, 5$$

$$C_{i1} = R_{i1}^2/3, \quad C_{i2} = R_{i2}^2/2, \ i = 1, 2$$

$$C_{i1} = \frac{\left[\ln\left(1 - R_{i1}\right)\right]^2}{100}, \quad i = 3, 4, 5$$

$$C_{i2} = \frac{\left[\ln\left(1 - R_{i2}\right)\right]^2}{60}, \quad i = 3, 4, 5$$

Note: R_{ij} is the reliability index of the jth unit in the ith subsystem, and C_{ij} is the cost of the jth unit in the ith subsystem.

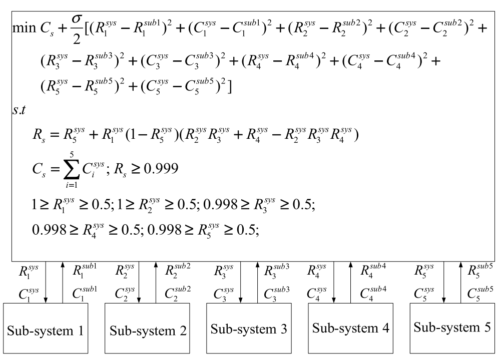

FIGURE 8. Optimization model by ATC-EPF.

TABLE 2. Comparison of AIO and ATC-EPF.

	AIO	ATC-EPF	Rate of deviation /%
C_S	1.1266	1.1155	0.98
R_S	0.9990	0.9987	0.03
R_1	0.5345	0.5351	0.11
R_2	0.5000	0.5004	0.08
R_3	0.5424	0.5425	0.01
R_4	0.9114	0.9099	0.16
R_5	0.9982	0.9980	0.02
C_1	0.4364	0.4357	0.16
C_2	0.4082	0.4085	0.07
C_3	0.0039	0.0040	2.56
C_4	0.0367	0.0360	1.91
C_5	0.2314	0.2312	0.08
R_{11}	0.8078	0.8081	0.03
R_{12}	0.6617	0.6615	0.03
R_{21}	0.7836	0.7808	0.36
R_{22}	0.6381	0.6411	0.47
R_{31}	0.4030	0.3989	1.02
R_{32}	0.2335	0.2493	2.48
R_{41}	0.7825	0.7871	0.59
R_{42}	0.5926	0.5933	0.12
R_{51}	0.9801	0.9838	0.38
R_{52}	0.8998	0.8884	1.27
Iterations	387	5	98.71

The above optimization problems can be decomposed into the ATC-EPF model according to Eqs. (6-8), as shown in Fig. 8 and the sub-systems are shown in Eqs. (10-14). Table 2 shows the comparison of the optimal value of AIO and ATC-EPF.

$$\begin{aligned}
&Subsystem1:\\
&\quad \min\ (R_1^{sys}-R_1^{sub1})^2+(C_1^{sys}-C_1^{sub1})^2\\
&\quad s.t\ R_1^{sub1}=R_{11}R_{12}\\
&\qquad C_1^{sub1}=\frac{R_{11}^2}{3}+\frac{R_{12}^2}{2}\\
&\qquad 0.5\le R_1^{sub1}\le 1.0\\
&\qquad 0.5\le R_{11}\le 0.98;\ 0.5\le R_{12}\le 0.98\\
&\qquad C_1^{sub1}\ge 0
\end{aligned}\tag{10}$$

$$\begin{aligned}
&Subsystem2:\\
&\quad \min\ (R_2^{sys}-R_2^{sub2})^2+(C_2^{sys}-C_2^{sub2})^2\\
&\quad s.t\ R_2^{sub2}=R_{21}R_{22}\\
&\qquad C_2^{sub2}=\frac{R_{21}^2}{3}+\frac{R_{22}^2}{2}\\
&\qquad 0.5\le R_2^{sub2}\le 1.0\\
&\qquad 0.5\le R_{21}\le 0.98;\quad 0.5\le R_{22}\le 0.98\\
&\qquad C_2^{sub2}\ge 0
\end{aligned}\tag{11}$$

$$\begin{aligned}
&Subsystem3:\\
&\quad \min\ (R_3^{sys}-R_3^{sub3})^2+(C_3^{sys}-C_3^{sub3})^2\\
&\quad s.t\ R_3^{sub3}=1-(1-R_{31})(1-R_{32})\\
&\qquad C_3^{sub3}=(\ln(1-R_{31}))^2/100+(\ln(1-R_{32}))^2/60\\
&\qquad 0.5\le R_3^{sub3}\le 0.998\\
&\qquad 0.2\le R_{31}\le 0.99;\quad 0.2\le R_{32}\le 0.99\\
&\qquad C_3^{sub3}\ge 0
\end{aligned}\tag{12}$$

$$\begin{aligned}
&Subsystem4:\\
&\quad \min\ (R_4^{sys}-R_4^{sub4})^2+(C_4^{sys}-C_4^{sub4})^2\\
&\quad s.t\ R_4^{sub4}=1-(1-R_{41})(1-R_{42})\\
&\qquad C_4^{sub4}=(\ln(1-R_{41}))^2/100+(\ln(1-R_{42}))^2/60\\
&\qquad 0.5\le R_4^{sub4}\le 0.998\\
&\qquad 0.2\le R_{41}\le 0.99;\ 0.2\le R_{42}\le 0.99\\
&\qquad C_4^{sub4}\ge 0
\end{aligned}\tag{13}$$

$$\begin{aligned}
&Subsystem5:\\
&\quad \min\ (R_5^{sys}-R_5^{sub5})^2+(C_5^{sys}-C_5^{sub5})^2\\
&\quad s.t\ R_5^{sub5}=1-(1-R_{51})(1-R_{52})\\
&\qquad C_5^{sub5}=(\ln(1-R_{51}))^2/100+(\ln(1-R_{52}))^2/60\\
&\qquad 0.5\le R_5^{sub5}\le 0.998\\
&\qquad 0.2\le R_{51}\le 0.99;\quad 0.2\le R_{52}\le 0.99\\
&\qquad C_5^{sub5}\ge 0
\end{aligned}\tag{14}$$

It is seen from Table 2 the rate of deviation via ATC-EPF compared with that of AIO is 0.02%-2.56%. Thus, the optimal solution obtained by ATC-EPF satisfied the accuracy in engineering practice. In addition, the iterations of ATC-EPF are 5 and AIO is 387, so the ATC-EPF is 77.4 times as much as AIO. That is, the computational efficiency of ATC-EPF is improved 98.71% compared with that of AIO. Therefore, the results show that the method presented in this paper is observably superior to the AIO.

IV. CONCLUSION

Analytical Target Cascading-based Exterior Penalty Function (ATC-EPF) is proposed to handle system optimization problems. The response bias of subsystem layer is introduced into the objective function of system through penalty factor according to the idea of objective level decomposition and coordination optimization. The optimization is decomposed into the master programming and the sub programming, and the solution scale of system is reduced.

The results are transferred to the master programming in the form of decoupled parameters after the independent optimization of each sub-programming. The master programming carries out global coordination optimization in accordance with the principle of overall system optimization, and sends the results to the sub-programming in the form of coordination parameters to coordinate the optimization activities of each subsystem. This method reflects the structural characteristics of the overall system and subsystem as well as subsystems. It is convenient for "parallel calculation" to further improve the efficiency and solves the difficulty of direct solution method, which is a practical method that can be popularized in engineering practices.

Two cases, that is, numerical and engineering examples, indicate that the optimal solution obtained by ATC-EPF is consistent with that of obtained by AIO, which verifies the accuracy. In addition, the computational efficiency of ATC-EPF is improved 95.97% and 98.71% compared with that of AIO in numerical and engineering examples. Thus, the method presented in this work is observably superior to the AIO method whether the computational efficiency or computational accuracy.

DECLARATION OF CONFLICTING INTERESTS

The authors declare that there is no conflict of interests regarding the publication of this article.

REFERENCES

[1] X. Luan, B. De Schutter, L. Meng, and F. Corman, ''Decomposition and distributed optimization of real-time traffic management for large-scale railway networks,'' *Transp. Res. B, Methodol.*, vol. 141, pp. 72–97, Nov. 2020, doi: 10.1016/j.trb.2020.09.004.

[2] I. Nizar, Y. Illoussamen, H. E. Ouarrak, E. H. Illoussamen, M. Grana, and M. Mestari, ''Safe and optimal navigation for autonomous multi-rotor aerial vehicle in a dynamic known environment by a decomposition-coordination method,'' *Cognit. Syst. Res.*, vol. 63, pp. 42–54, Oct. 2020, doi: 10.1016/j.cogsys.2020.05.003.

[3] D. Zhou, S. Wang, and H. Gao, ''Study on multi-scale coupled ecological dispatching model based on the decomposition-coordination principle,'' *Water*, vol. 11, no. 7, p. 1443, Jul. 2019, doi: 10.3390/w11071443.

[4] J. Li, B. Lu, Z. Wang, and M. Zhu, ''Bi-level optimal planning model for energy storage systems in a virtual power plant,'' *Renew. Energy*, vol. 165, pp. 77–95, Mar. 2021, doi: 10.1016/j.renene.2020.11.082.

[5] A. Engelmann, Y. Jiang, B. Houska, and T. Faulwasser, ''Decomposition of nonconvex optimization via bi-level distributed ALADIN,'' *IEEE Trans. Control Netw. Syst.*, vol. 7, no. 4, pp. 1848–1858, Dec. 2020, doi: 10.1109/TCNS.2020.3005079.

[6] F. D. R. Machado, A. L. Diniz, C. L. T. Borges, and L. C. Brandão, ''Asynchronous parallel stochastic dual dynamic programming applied to hydrothermal generation planning,'' *Electr. Power Syst. Res.*, vol. 191, Feb. 2021, Art. no. 106907, doi: 10.1016/j.epsr.2020.106907.

[7] M. A. Aydin and Z. C. Taákin, ''Decentralized decomposition algorithms for peer-to-peer linear optimization,'' *Oper. Res.*, vol. 54, no. 6, pp. 1835–1861, Nov. 2020, doi: 10.1051/ro/2019097.

[8] T. Yang and Y. Yu, ''Security region-based laminar flow coordinated optimization of grids,'' *Int. J. Electr. Power Energy Syst.*, vol. 124, Jan. 2021, Art. no. 106406, doi: 10.1016/j.ijepes.2020.106406.

[9] X. Zhou, Y. Li, C. Bu, T. Zhang, H. Lin, and J. Yi, ''Demand side response participation in reserve configuration optimization based on decomposition and coordination,'' *IEEE Access*, vol. 8, pp. 65046–65059, 2020, doi: 10.1109/ACCESS.2020.2983868.

[10] N. F. Avila and C.-C. Chu, ''Distributed probabilistic ATC assessment by optimality conditions decomposition and LHS considering intermittent wind power generation,'' *IEEE Trans. Sustain. Energy*, vol. 10, no. 1, pp. 375–385, Jan. 2019, doi: 10.1109/TSTE.2018.2796102.

[11] X. Li, X. Wang, H. Zhang, and Y. Guo, ''Trajectory optimization using analytical target cascading,'' *J. Mech. Des.*, vol. 139, no. 12, Dec. 2017, Art. no. 124501, doi: 10.1115/1.4037714.

[12] A.-B. Liu, P. B. Luh, M. A. Bragin, and B. Yan, ''Ordinal-optimization concept enabled decomposition and coordination of mixed-integer linear programming problems,'' *IEEE Robot. Autom. Lett.*, vol. 5, no. 4, pp. 5051–5058, Oct. 2020, doi: 10.1109/LRA.2020.3005125.

[13] P. Liu, Z. Cai, P. Xie, X. Li, and Y. Zhang, ''A decomposition-coordination planning method for flexible generation resources in isolated microgrids,'' *IEEE Access*, vol. 7, pp. 76720–76730, 2019, doi: 10.1109/ACCESS.2019.2922756.

[14] X. Zhang, H.-Z. Huang, Z. Wang, Y. Liu, and Y. Li, ''A Pareto set coordination method for analytical target cascading,'' *Concurrent Eng.*, vol. 21, no. 4, pp. 286–295, Dec. 2013, doi: 10.1177/1063293X13499358.

[15] H. M. Kim, N. F. Michelena, P. Y. Papalambros, and T. Jiang, ''Target cascading in optimal system design,'' *J. Mech. Des.*, vol. 125, no. 3, pp. 474–480, Sep. 2003, doi: 10.1115/1.1582501.

[16] S. Huang, Q. Wu, J. Zhao, and W. Liao, ''Distributed optimal voltage control for VSC-HVDC connected large-scale wind farm cluster based on analytical target cascading method,'' *IEEE Trans. Sustain. Energy*, vol. 11, no. 4, pp. 2152–2161, Oct. 2020, doi: 10.1109/TSTE.2019.2952122.

[17] P. L. Du, Z. Chen, Y. X. Chen, Z. W. Ma, and H. G. Ding, ''A Bi-level linearized dispatching model of active distribution network with multi-stakeholder participation based on analytical target cascading,'' *IEEE Access*, vol. 7, pp. 154844–154858, 2019, doi: 10.1109/ACCESS.2019.2949097.

[18] S. F. Alyaqout and A. F. Alyaqout, ''Control of a nonlinear system utilizing analytica target cascading,'' *J. Eng. Res.*, vol. 8, no. 2, pp. 286–303, 2020.

[19] P. Guarneri, M. Gobbi, and P. Y. Papalambros, ''Efficient multi-level design optimization using analytical target cascading and sequential quadratic programming,'' *Structural Multidisciplinary Optim.*, vol. 44, no. 3, pp. 351–362, Sep. 2011, doi: 10.1007/s00158-011-0630-2.

[20] J. Chen, Y. Wu, L. Zhang, X. He, and S. Dong, ''Dynamic optimization design of the suspension parameters of car body-mounted equipment via analytical target cascading,'' *J. Mech. Sci. Technol.*, vol. 34, no. 5, pp. 1957–1969, May 2020, doi: 10.1007/s12206-020-0417-8.

[21] T. Cui, W. Zhao, C. Wang, Y. Guo, and H. Zheng, ''Design optimization of a steering and suspension integrated system based on dynamic constraint analytical target cascading method,'' *Struct. Multidisciplinary Optim.*, vol. 62, no. 1, pp. 419–437, Jul. 2020, doi: 10.1007/s00158-019-02472-8.

[22] N. Kang, M. Kokkolaras, P. Y. Papalambros, S. Yoo, W. Na, J. Park, and D. Featherman, ''Optimal design of commercial vehicle systems using analytical target cascading,'' *Struct. Multidisciplinary Optim.*, vol. 50, no. 6, pp. 1103–1114, Dec. 2014, doi: 10.1007/s00158-014-1097-8.

[23] J. Zheng, L. Gao, H. Qiu, X. Shao, and P. Jiang, ''Variable fidelity metamodel-based analytical target cascading method for green design,'' *Int. J. Adv. Manuf. Technol.*, vol. 87, nos. 5–8, pp. 1203–1216, Nov. 2016, doi: 10.1007/s00170-012-4705-z.

[24] P. Jiang, J. Wang, Q. Zhou, and X. Zhang, ''An enhanced analytical target cascading and Kriging model combined approach for multidisciplinary design optimization,'' *Math. Problems Eng.*, vol. 2015, pp. 1–11, Jan. 2015, doi: 10.1155/2015/685958.

[25] Z. Jiang, H. Qiu, M. Zhao, S. Zhang, and L. Gao, ''Analytical target cascading using ensemble of surrogates for engineering design problems,'' *Eng. Computations*, vol. 32, no. 7, pp. 2046–2066, Oct. 2015, doi: 10.1108/EC-11-2014-0242.

[26] T. Qu, X. D. Chen, Y. Zhang, H. Yang, and G. Q. Huang, ''Analytical target cascading-enabled optimal configuration platform for production service systems,'' *Int. J. Comput. Integr. Manuf.*, vol. 24, no. 5, pp. 457–470, May 2011, doi: 10.1080/0951192X.2010.551282.

[27] W. S. Wang, V. Y. Blouin, M. K. Gardenghi, G. M. Fadel, M. M. Wiecek, and B. C. Sloop, ''Cutting plane methods for analytical target cascading with augmented Lagrangian coordination,'' *J. Mech. Des.*, vol. 135, no. 10, 2013, Art. no. 104502, doi: 10.1115/1.4024847.

[28] A. Mohammadi and A. Kargarian, ''Accelerated and robust analytical target cascading for distributed optimal power flow,'' *IEEE Trans. Ind. Informat.*, vol. 16, no. 12, pp. 7521–7531, Dec. 2020, doi: 10.1109/TII.2020.2973213.

[29] H. Pan, M. Ding, R. Bi, and L. Sun, ''Research on cooperative planning of distributed generation access to AC/DC distribution (Micro) grids based on analytical target cascading,'' *Energies*, vol. 12, no. 10, 2019, Art. no. 1847, doi: 10.3390/en12101847.

[30] Y. D. Jung, N. Kang, and I. Lee, ''Modified augmented Lagrangian coordination and alternating direction method of multipliers with parallelization in non-hierarchical analytical target cascading,'' *Struct. Multidisciplinary Optim.*, vol. 58, no. 2, pp. 555–573, 2018, doi: 10.1007/s00158-018-1907-5.

[31] S. DorMohammadi and M. Rais-Rohani, ''Exponential penalty function formulation for multilevel optimization using the analytical target cascading framework,'' *Struct. Multidisciplinary Optim.*, vol. 47, no. 4, pp. 599–612, Apr. 2013, doi: 10.1007/s00158-012-0861-x.

[32] S. Tosserams, M. Kokkolaras, L. F. P. Etman, and J. E. Rooda, ''A nonhierarchical formulation of analytical target cascading,'' *J. Mech. Des.*, vol. 132, no. 5, May 2010, Art. no. 051002, doi: 10.1115/1.4001346.

[33] Y. Kim and J. Lee, ''Probabilistic optimization of engine mount to enhance vibration characteristics using first-order reliability-based target cascading,'' *J. Vibrat. Control*, vol. 27, nos. 7–8, pp. 759–773, Apr. 2021, doi: 10.1177/1077546320933474.

[34] J. Han and P. Y. Papalambros, ''A note on the convergence of analytical target cascading with infinite norms,'' *J. Mech. Design*, vol. 132, no. 3, Mar. 2010, doi: 10.1115/1.4001001.

[35] F. Xiong, X. Yin, W. Chen, and S. Yang, ''Enhanced probabilistic analytical target cascading with application to multi-scale design,'' *Eng. Optim.*, vol. 42, no. 6, pp. 581–592, Jun. 2010, doi: 10.1080/03052150903386682.

[36] G. T. Jiang, M. Zhu, and Z. Wu, ''Reliability allocation using probabilistic analytical target cascading with efficient uncertainty propagation,'' *Eksploatacja Niezawodnosc-Maintenance Rel.*, vol. 14, no. 4, pp. 270–277, 2012.

[37] Q. Ouyang, X. Chen, and W. Yao, "Sequential probabilistic analytical target cascading method for hierarchical multilevel optimization under uncertainty," *Structural Multidisciplinary Optim.*, vol. 49, no. 2, pp. 267–280, Feb. 2014, doi: 10.1007/s00158-013-0967-9.

[38] Q. Ouyang, W. Yao, and X. Chen, "Mixed uncertainty based analytical target cascading: An approach for hierarchical multilevel optimization under probabilistic and interval mixed uncertainties," *Struct. Multidisciplinary Optim.*, vol. 57, no. 4, pp. 1475–1493, Apr. 2018, doi: 10.1007/s00158-017-1820-3.

[39] Y. Jung, J. Lee, M. Lee, N. Kang, and I. Lee, "Probabilistic analytical target cascading using kernel density estimation for accurate uncertainty propagation," *Struct. Multidisciplinary Optim.*, vol. 61, no. 5, pp. 2077–2095, May 2020, doi: 10.1007/s00158-019-02455-9.

[40] W. Li, M. Xiao, Y. Yi, and L. Gao, "Maximum variation analysis based analytical target cascading for multidisciplinary robust design optimization under interval uncertainty," *Adv. Eng. Informat.*, vol. 40, pp. 81–92, Apr. 2019, doi: 10.1016/j.aei.2019.04.002.

BIN BAI received the Ph.D. degree in mechanical engineering from Beihang University, Beijing, China. He is currently an Associate Professor. He has published more than 30 articles which are indexed by SCI, such as *Aerospace Science and Technology*, *Information Sciences*, *Expert Systems with Applications*, *Applied Mathematical Modelling*, *Computers & Industrial Engineering*, *Journal of Aerospace Engineering*, *Journal of Sound and Vibration*, and *Journal of Mechanisms and Robotics* (ASME). His main research interests include system dynamics; aeroengine vibration, strength, reliability, and robustness design; and reliability assessment of industrial robots.

CHUXIONG XIE received the master's degree in physical electronics from Zhejiang Normal University. He currently works with the Intelligent Manufacturing College. His research interests include intelligent manufacturing, automatic control, and vocational education.

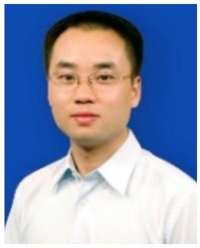

XIANGDONG LIU received the master's degree in software engineering from Central South University. He is currently an Associate Professor. He was with the ICAN Contest of College Students' Innovative Entrepreneurial Expert Judges. He holds one national invention patent and three utility model patents. He was awarded the Technical Expert of China Construction Machinery Industry and the Evaluation and Consultation Expert of Changsha Vocational Ability Construction Project.

WEI LI received the master's degree in mechanical engineering from the China University of Mining and Technology. He is currently an Engineer and a Lecturer. His research interests include construction machinery hydraulics and mechanical structure design. He is the Database Expert of skill competition in Hunan Province.

WEIYU ZHONG received the master's degree in mechanical manufacturing and automation from the Nanjing University of Science and Technology, Jiangsu, China. His research interests include system reliability theory, reliability algorithm, and analysis.